Two-channel Image Dehazing Algorithm Based on the Improved Guided Filter for Intelligent Automobile

Ping Liu
College of Automation
Chongqing University of Posts and Telecommunications
Chongqing, China
email: liuping_cqupt@cqupt.edu.cn

Yang Luo
College of Automation
Chongqing University of Posts and Telecommunications
Chongqing, China
email: s200331121@stu.cqupt.edu.cn

Mingjie Liu
College of Automation
Chongqing University of Posts and Telecommunications
Chongqing, China
email: liumj@cqupt.edu.cn

Changhao Piao
College of Automation
Chongqing University of Posts and Telecommunications
Chongqing, China
email: piaoch@cqupt.edu.cn

***Abstract* —** This work proposes a two-channel image dehazing strategy based on threshold segmentation. The algorithm first uses the Otsu threshold method to segment the sky and the background, and then estimates the dark channel and bright channel atmospheric light values of the sky and background respectively, and uses a weighting function to fuse them, and finally obtains the accurate mixed atmospheric light of each area. In order to improve the detail effect of the restored image, an improved guided filtering technique is proposed to further process the obtained transmission image. Experiment tests show the performance of the proposed method.

Keywords—*Prior Theory; Image-Dehazing; Otsu-Thresholding; Two-Channel Estimation; Guided Filtering*

I. INTRODUCTION

With the development of image technique, various outdoor vision systems based on machine vision have played increasingly important roles in our daily life [1, 2]. However, the outdoor vision system often affects the operation of the entire system due to the interference of meteorological weather such as smog, which has laid a great hidden danger to the safety and property. High quality images are the prerequisite for the stable operation of a vision system and an important factor in intelligent automobile system. According to previous studies [3], image dehazing algorithms can be divided into following types [4, 5]: priori theory-based image dehazing algorithms, image enhancement-based image dehazing algorithms, deep learning-based image dehazing algorithms. Although the end-to-end deep learning-based single-stage dehazing methods have good dehazing effect, these methods rely too much on the simulation data sets and the parameters of trained neural network are different, which lead to poor dehazing effect on real foggy scenes.

This work was supported by National key R&D program (No.2022YFE0101000), the Chongqing Natural Science Foundation Project (CSTB2022NSCQ-MSX0355) and Chongqing Technology Innovation and Application Development Project (cstc2020jscx-msxmX0181).

To further explore a realistic and effective image dehazing strategy, this paper deeply studies the physical model-based image dehazing algorithm and combines the advantages and disadvantages of the current research algorithms. Correspondingly, a dual-channel image dehazing method based on threshold segmentation and improved guided filter is proposed in this work, where the atmospheric light value estimation formula is improved so as to avoid the defects of the existing mainstream methods. Furthermore, the mainstream test atlas RESIDE is employed for testing and the reference methods are employed for comparative analysis.

II. TWO CHANNEL THEORY-BASED COMPUTATION

A. Threshold-based Image Division

Briefly, the key point of calculating the foggy image by using the atmospheric scattering model is to simulate the physical degradation of foggy images based on the Mie atmospheric scattering theory. Generally, the related process is shown in Fig. 1.

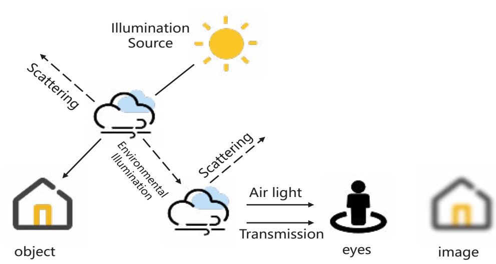

Fig. 1. Principles of atmospheric scattering imaging

On the basis of the mathematical model (ASM) proposed by Huang et al. [6], the mathematical description is stated as follows:

$$I(x) = J(x)t(x) + A(x)(1 - t(x)) \quad (1)$$

where x represents the pixel position of the image, $I(x)$ is the foggy image, $J(x)$ is a clear fog-free image, and $A(x)$ is an atmospheric light value. Therefore, the core of physical model-based image dehazing is to obtain the atmospheric light value $A(x)$ and transmittance $t(x)$.

Since the white and highlighted parts of the image background will influence the calculation results of dark channel prior (DCP) theory and bright channel prior (BCP) theory [7], this work employs the Otsu threshold method [8] to segment the sky, the white/highlighted parts and the background of the image, and then to calculate the corresponding atmospheric light value and transmittance. Correspondingly, the sky part and the background can be presented as follows:

$$\begin{cases} I_{sky}(x) = I(x)I_{\_sky} \\ I_{black}(x) = I(x)I_{\_black} \end{cases} \quad (2)$$

where $I_{sky}(x)$ is the sky part and $I_{black}(x)$ is the background, $I_{\_sky}$ and $I_{\_black}$ are the corresponding threshold matrices by using the Otsu threshold method.

B. Two Channel Calculation

With using the results of image division, two minimum operations are executed on the sky part to get the corresponding dark channel image,

$$I_{sky}^{dark}(x) = \min_{y \in \Omega(x)} \left(\min_{c \in \{R,G,B\}} I_{sky}(x) \right) \quad (3)$$

where $\Omega(x)$ is the filter window of the maximum filter. Accordingly, sorting the images of $I_{sky}^{dark}(x)$ in descending order, and select the first 0.1% of the pixels for the next calculation:

$$A_{sky} = \frac{1}{s} \sum_{x=1}^{s} M_{sky}^{dark}(x) \quad (4)$$

where s is the sum of the first 0.1% pixels, $M_{sky}^{dark}(x)$ is the result of $I_{sky}^{dark}(x)$ after sorting in descending order.

Meanwhile, based on the theory of BCP, the partial atmospheric light value estimation formula can be calculated by the following equation,

$$A^{light}(x) = \max_{y \in \Omega(x)} \left(\max_{c \in \{R,G,B\}} I^c(y) \right) \quad (5)$$

where $I^c(y)$ is the RGB foggy image, x is the center pixel, and $\Omega(x)$ is the filter window of the maximum filter. Finally, an improved atmospheric light value estimation formula is proposed in this work as follows,

$$A(x) = \alpha A^{light}(x) + \beta A_{sky} \quad (6)$$

In Eq. (6), the parameters α and β are recommended as 0.75 and 0.2, respectively.

Furthermore, the DCP theory is also employed to solve the atmospheric scattering model. The mathematical description of the dark channel prior theory using in this work is stated as follows:

$$t(x) = 1 - 0.95 \min_{y \in \Omega(x)} \left(\min_{c \in \{R,G,B\}} \frac{I^c(y)}{A^c} \right) \quad (7)$$

where A^c is the RGB atmospheric light value.

III. Guided Filtering

On the basis of two channel computation, an improved guided filtering method is proposed, the core of the filtering method is to retain the dehazing information in the transmittance map by means of linear transformation, and relying on the dehazing information to guide the grayscale image of the input image to perform dehazing filtering. The process of this method is shown in Fig. 2.

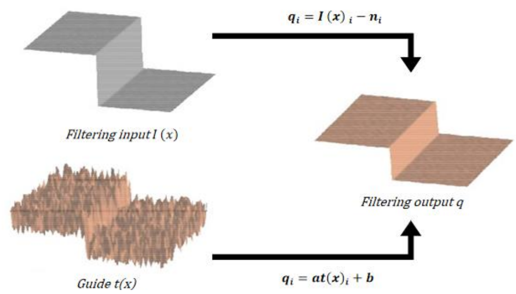

Fig. 2. Process of improved guided filtering method

Assume that there is a local linear relationship between the guide image $t(x)$ and the output image q within the filtering window w_k,

$$q_i = a_k t(x)_i + b_k, \forall i \in w_k \quad (8)$$

Accordingly, a_k and b_k is calculated by,

$$a_k = \frac{\mathrm{cov}(t(x)_k, I(x)_k)}{\mathrm{var}(t(x)_k) + \varepsilon} \quad (9)$$

$$b_k = \bar{I}_k - a\bar{t}(x)_k \quad (10)$$

where ε is a regularization parameter, $\bar{I}_k = \frac{1}{|w|} \sum_{i \in w_k} I(x)_i$, $\bar{t}(x)_k = \frac{1}{|w|} \sum_{i \in w_k} t(x)_i$.

Therefore, the filtered transmittance is calculated by the following equation,

$$t_f(x) = q = at(x) + b \quad (11)$$

And the final dehazing formula can be described as,

$$J(x) = \frac{I(x) - A(x)}{\max(t_f(x), T_0)} + A(x) \quad (12)$$

where T_0 is the threshold value.

IV. Algorithm Implementation

Briefly, the implementation of the proposed method is shown in Fig. 3, the detailed steps are given as follows.

- **Step 1**: Use the Otsu threshold method to divide the input image into two parts and obtain the dark channel image and the light channel image of the input image at the same time;

- **Step 2**: Solve the global atmospheric light A_{sky} for the sky part, and use the light channel image to obtain the regional atmospheric light value $A_{light}(x)$;
- **Step 3**: Use a weighted method to mix the two atmospheric light values in step 2 to obtain the final mixed atmospheric light value $A(x)$;
- **Step 4:** Obtain transmittance images with the help of dark channel images and mixed atmospheric light values;
- **Step 5**: Conduct guided filtering on the transmittance image, and use the atmospheric scattering physical model to solve the haze-free background;
- **Step 6:** The fog-free background is fused with the sky segmented in step 1 to obtain the final dehazed image.

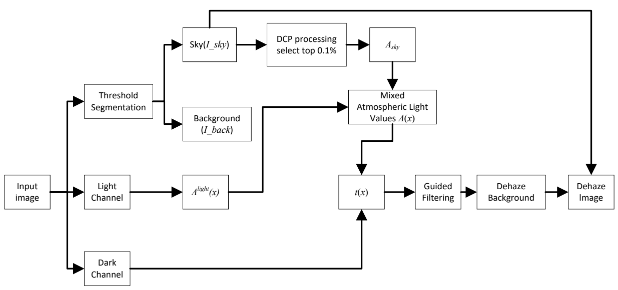

Fig. 3. Process of proposed algorithm

V. Experimental Tests

The mainstream image set Realistic Single Image Dehazing (RESIDE) [2] is employed for testing. Meanwhile, the dark channel prior dehazing algorithm [1], DEFADE algorithm [9] and adaptive bilateral weakening dehazing method [10] are employed for comparison. The partial illustrations are given in Fig. 4. It can be found that the four methods are efficient to deal with the foggy sky image. However, there is more or less distortion in some parts, and the algorithm proposed in this paper avoids this problem. At the same time, the dehazing effect of the algorithm in this paper is also in the forefront of these three categories. The overall dehazing effect is better, and the detail retention and highlighting are the strongest. Taking the second column of images as an example, it can be clearly found that the proposed algorithm shows the dark details in the lower right corner, and other algorithms do not work well with this detail, which revealing the effectiveness of the proposed strategy.

Meanwhile, the widely used performance indexes, including the aware density evaluator (FADE), natural image quality evaluator (NIQE), structural similarity (SSIM), peak signal noise ratio (PSNR), mean squared error (MSE) are adopted for performance comparison. Results comparison is shown in Table 1. It is obvious that the proposed method owns good performances. These results show that the proposed method can be further combined into the computation network [11].

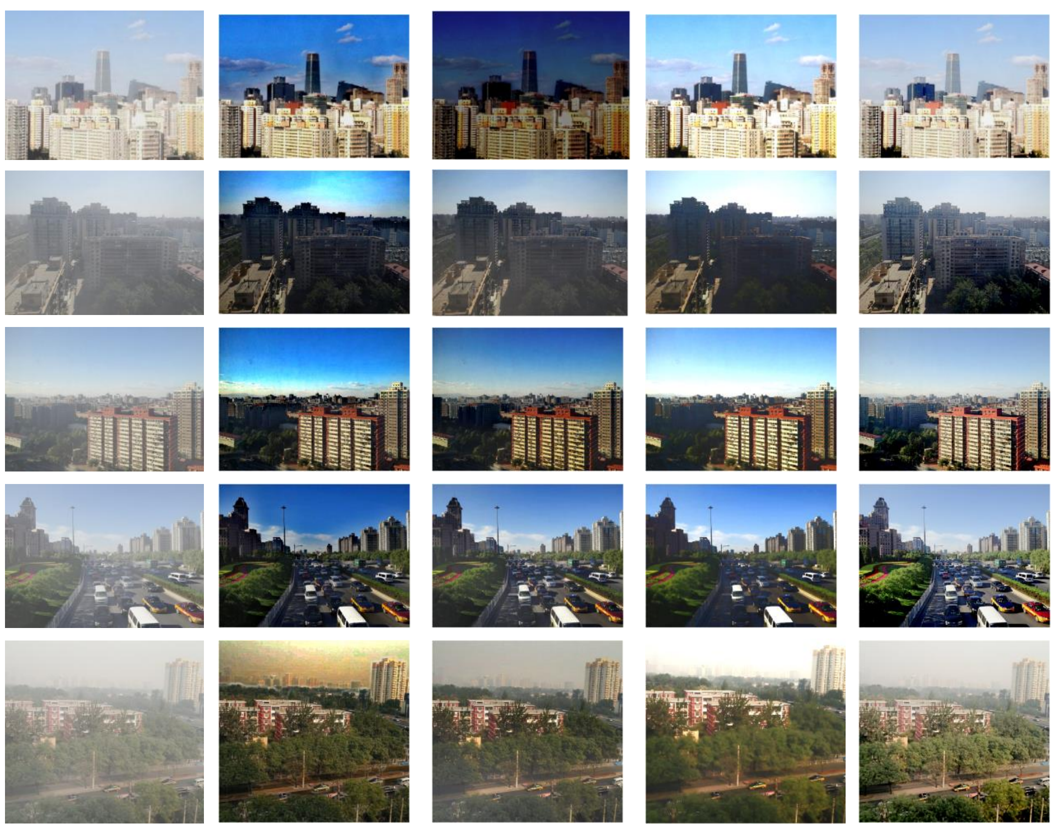

(a) Original image (b) He [1] (c) DEFADE [9] (d) Bilateral [10] (e) Current work

Fig. 4. Comparison of different methods

TABLE 1. PERFORMANCE INDEX RESULTS OF DIFFERENT METHODS

Image NO.	Algorithm	PSNR	MSE	SSIM	FADE	NIQE
2	He [1]	14.81	2148	0.8466	**0.2809***	2.7145
	DEFADE [9]	19.6728	701.1323	0.9053	1.0623	2.4746
	Bilateral [10]	20.9662	520.5511	0.7612	1.3115	2.6576
	Current work	**24.2158***	**246.3182***	**0.9458***	0.4841	**2.3609***
4	He [1]	11.8247	4271	0.9231	0.2552	3.1512
	DEFADE [9]	6.0843	10620	0.5341	**0.2433***	3.1268
	Bilateral [10]	22.3177	381.3382	0.929	0.6021	**2.9764**
	Current work	**27.3452***	**119.829***	**0.9796***	0.7643	3.0832
5	He [1]	14.8874	2110	0.8753	**0.2858***	3.3
	DEFADE [9]	2.8966	18772	0.8829	0.4191	2.8966
	Bilateral [10]	21.3376	477.883	0.8729	0.7523	2.3452
	Current work	**24.2973***	**241.7433***	**0.9572***	0.7377	**2.2504***
43	He [1]	17.9879	1033	0.9067	**0.1560***	2.7625
	DEFADE [9]	17.7077	1102	0.8823	0.339	2.5839
	Bilateral [10]	17.1696	1247	0.7781	0.2801	2.5102
	Current work	**22.87788***	**335.1985***	**0.9507***	0.2705	**2.4923***
179	He [1]	20.55773	571.93	0.9059	**0.2016***	2.8953
	DEFADE [9]	**21.484***	**462.04***	0.9146	0.4035	2.1976
	Bilateral [10]	19.1363	793.3199	0.8339	0.3647	2.8096
	Current work	20.5105	578.1314	**0.9473***	0.4034	**2.1404***

To further verify the performance of the proposed method, 30 images of different scenes and fog concentrations from the RESIDE atlases are chosen for testing. The NIQE and FADE performance indexes of the experiment test are given in Fig. 5 and Fig. 6. It can be seen that the proposed algorithm has great advantage over other algorithms in most cases. The average PSNR is above 22, and the average SSIM is also higher than 0.90. From the perspective of stability, the algorithm of this paper performance good. However, other algorithms, such as the DEFADE algorithm, show a large trough in the PSNR value in the image No. 5, and the PSNR even drops below 4, further showing the efficiency of the proposed improvement.

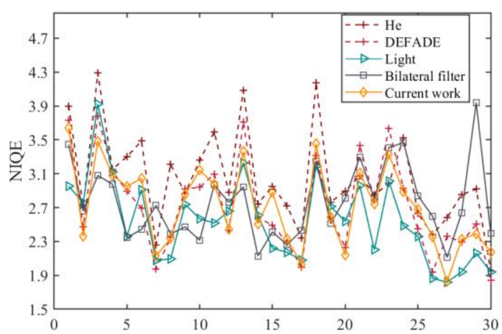

Fig. 5. NIQE performance indexes of the experiment test

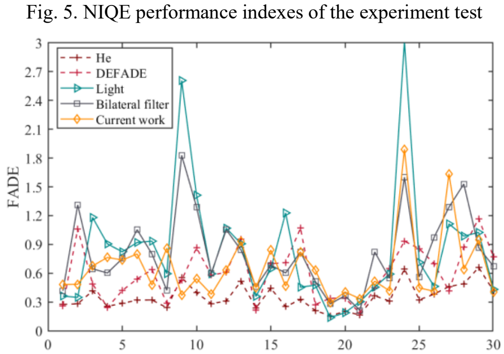

Fig. 6. FADE performance indexes of the experiment test

VI. CONCLUSION

The research object of this paper is the image dehazing algorithm in outdoor scenes, which can improve the reliability of the visual system in foggy conditions. An improved image dehazing algorithm based on atmospheric scattering model is proposed to further improve the performance of image dehazing. Combining subjective evaluation and objective evaluation, the proposed algorithm has great advantages over other algorithms. In terms of subjective evaluation, it not only avoids the phenomenon of sky distortion, but also improves the details of some shadows, and the dehazing effect is obvious; in terms of objective evaluation, the PSNR, MSE and SSIM indicators of the image are efficiently improved when compared with other algorithms. In terms of NIQE and FADE, in the non-large area dense fog scene, it still has certain advantages over other algorithms, the performance is stable, and the indicators performance good. Experiment tests show the practical application value of the proposed method.

REFERENCES

[1] Y. Liu, L. Guo, H. Gao, Z. You, and B. Zhang, "Machine vision based condition monitoring and fault diagnosis of machine tools using information from machined surface texture: A review," *Mechanical Systems Signal Processing,* vol. 164, no. 11, p. 108068, 2022.

[2] J. Zhou and J. Yu, "Chisel edge wear measurement of high-speed steel twist drills based on machine vision," *Computers in Industry,* vol. 128, p. 103436, 2021.

[3] H. Huang, K. Wu, J. Song, H. Wang, F. Ru, and L. Guo, "A dark channel image dehazing algorithm based on the fusion of global and regional airlight," *Journal of Nanjing University(Natural Sciences),* vol. 57, no. 4, pp. 551-565, 2021.

[4] A. S. Parihar, Y. K. Gupta, Y. Singodia, V. Singh, and K. Singh, "A Comparative Study of Image Dehazing Algorithms," in *2020 5th International Conference on Communication and Electronics Systems (ICCES)*, 2020.

[5] L. Li, Y. Dong, W. Ren, J. Pan, C. Gao, N. Sang, *et al.*, "Semi-Supervised Image Dehazing," *IEEE Transactions on Image Processing,* vol. 29, pp. 2766-2779, 2020.

[6] D. Huang, W. Wang, J. Lu, and K. Chen, "Fast Single Image Haze Removal Method based on Atmospheric Scattering Model - ScienceDirect," *IFAC-PapersOnLine,* vol. 51, no. 17, pp. 211-216, 2018.

[7] K. He, J. Sun, and X. Tang, "Single image haze removal using dark channel prior," *IEEE transactions on pattern analysis machine intelligence,* vol. 33, no. 12, pp. 2341-2353, 2010.
[8] J. Chao, Y. Xiaoxiao, and W. Xiaohai, "Algorithm of Double Threshold Image Segmentation Combined QGA with Two-Dimensional Otsu," in *2020 5th International Conference on Mechanical, Control and Computer Engineering (ICMCCE)*, 2020.
[9] L. K. Choi, J. You, and A. C. J. I. T. o. I. P. Bovik, "Referenceless prediction of perceptual fog density and perceptual image defogging," vol. 24, no. 11, pp. 3888-3901, 2015.
[10] B. Zhang and J. Allebach, "Adaptive bilateral filter for sharpness enhancement and noise removal," vol. 17, no. 5, pp. 664-678, 2008.
[11] B. Liu, Z. Yan, and C. Chen, "Medium Access Control for Wireless Body Area Networks with QoS Provisioning and Energy Efficient Design," *IEEE Transactions on Mobile Computing*, Vol. 16, No. 2, pp. 422-434, 2017.